Altered cortical and subcortical local coherence in obstructive sleep apnea: a functional magnetic resonance imaging study

EMILIANO SANTARNECCHI[1,2], ISABELLA SICILIA[1,2], JONAS RICHIARDI[3], GIAMPAOLO VATTI[1], NICOLA RICCARDO POLIZZOTTO[4], DANIELA MARINO[1,2], RAFFAELE ROCCHI[1,2], DIMITRI VAN DE VILLE[3] and ALESSANDRO ROSSI[1]

[1]Department of Neurological and Sensorial Sciences, University of Siena, Siena, Italy, [2]Center for Sleep medicine, University of Siena, Siena, Italy, [3]Medical Image Processing Laboratory, Ecole Polytechnique Fédérale de Lausanne and University of Geneva, Lausanne, Switzerland, and [4]Department of Psychiatry, University of Pittsburgh, Pittsburgh, PA, USA

SUMMARY

Obstructive sleep apnea (OSA) syndrome is the most common sleep-related breathing disorder, characterized by excessive snoring and repetitive apneas and arousals, which leads to fragmented sleep and, most importantly, to intermittent nocturnal hypoxaemia during apneas. Considering previous studies about morphovolumetric alterations in sleep apnea, in this study we aimed to investigate for the first time the functional connectivity profile of OSA patients and age–gender–matched healthy controls, using resting-state functional magnetic resonance imaging (fMRI). Twenty severe OSA patients (mean age 43.2 ± 8 years; mean apnea–hypopnea index, 36.3 h^{-1}) and 20 non-apneic age–gender–body mass index (BMI)-matched controls underwent fMRI and polysomnographic (PSG) registration, as well as mood and sleepiness evaluation. Cerebro-cerebellar regional homogeneity (ReHo) values were calculated from fMRI acquisition, in order to identify pathology-related alterations in the local coherence of low-frequency signal (<0.1 Hz). Multivariate pattern classification was also performed using ReHo values as features. We found a significant pattern of cortical and subcortical abnormal local connectivity in OSA patients, suggesting an overall rearrangement of hemispheric connectivity balance, with a decrease of local coherence observed in right temporal, parietal and frontal lobe regions. Moreover, an increase in bilateral thalamic and somatosensory/motor cortices coherence have been found, a finding due possibly to an aberrant adaptation to incomplete sleep–wake transitions during nocturnal apneic episodes, induced by repetitive choke sensation and physical efforts attempting to restore breathing. Different hemispheric roles into sleep processes and a possible thalamus key role in OSA neurophysiopathology are intriguing issues that future studies should attempt to clarify.

INTRODUCTION

Obstructive sleep apnea syndrome (OSA) is a very common sleep disorder, the neuropathophysiology of which remains controversial (Horner, 2008) . It is characterized by excessive snoring and repetitive nocturnal apneas and arousals, which leads to fragmented sleep and, most importantly, intermittent nocturnal hypoxaemia during apneas. These result in a complex and disabling condition composed by daytime sleep-iness, neurocognitive problems such as deficits in memory, attention and visuoconstructive abilities (Bruin and Bagnato, 2010), reduced work performance and a worsening of overall quality of life (Bulcun *et al.*, 2012). During the last 15 years several brain alterations have also been documented. The majority of studies, performed through voxel-based morphometry (VBM) or surface-based parcellation approaches, have highlighted grey matter concentration differences in both cortical and subcortical brain regions, with hippocampus,

parahippocampal gyrus, fronto-parietal cortices, temporal lobe, anterior cingulate and cerebellum as the most targeted regions (Joo *et al.*, 2010; Macey *et al.*, 2008; Torelli *et al.*, 2011; Zimmerman and Aloia, 2006). Moreover, studies performed with diffusion tensor imaging (DTI) supported the evidence of a widespread white matter integrity alteration that includes axons linking major structures within the limbic system, pons, frontal, temporal and parietal cortices and projections to and from the cerebellum (Macey *et al.*, 2008).

Functional imaging has also been explored extensively, and the results suggest an intrinsic neural reorganization that may explain the neuropsychological deterioration in OSA patients. For instance, a functional magnetic resonance imaging (fMRI) study from (Ayalon *et al.* (2006) suggested the recruitment of additional brain areas during learning and memory tasks in OSA patients compared to control subjects, reflecting an adaptive compensatory recruitment response. This hypothesis is consistent with dynamic, compensatory changes in terms of increased brain activity, seen after sleep deprivation in healthy subjects (Drummond *et al.*, 2000). Moreover, a positron emission tomography (PET) study suggests a right-lateralized decrease in brain metabolism with the involvement of precuneus, middle and posterior cingulate gyrus, parieto–occipital cortex and prefrontal cortex (Yaouhi *et al.*, 2009). A spectroscopy study additionally revealed a decrease of N-acetylaspartate to creatine (NAA/Cr) ratios in frontal lobe grey and white matter, associated with an increase in thalami choline (Cho)/Cr ratios compared to control subjects (Algin *et al.*, 2012). Finally, even though possible communalities between sleep disorders brain alterations and the excessive daytime sleepiness feature of several neurodegenerative disorders have already been suggested (Gama *et al.*, 2010), surprisingly there have been few studies in OSA patients about structural/functional alterations of sleep-related deep brain structures such as hypothalamus, pons, midbrain and several cerebellar regions.

These results suggest that the OSA condition has a great impact on brain structure and functionality, but little is known about potential compensatory mechanisms and their representation at a whole brain network level. From this viewpoint, canonical task-based fMRI and PET studies could be inadequate to resolve the issue considering former stimulus dependency and the latter low spatial resolution.

Functional magnetic resonance imaging during resting condition (rs-fMRI) is a non-invasive high-resolution technique for examining brain functioning. It utilizes the dependency between the spontaneous blood oxygen level-dependent (BOLD) signal fluctuation of different brain regions to identify broadly connected networks at high spatial resolution. In this study we attempted to characterize OSA and age–gender–body mass index (BMI)-matched healthy controls by their functional connectivity profile, using a recently developed approach called 'regional homogeneity' (ReHo) (Zang *et al.*, 2004) to investigate local coherence of fMRI data. ReHo is a data-driven method developed to analyse resting-state data at single-voxel level, based on the assumption that the

haemodynamic characteristics of each voxel within a functional cluster are similar and/or synchronous, and the haemodynamic characteristics of each are modulated in parallel under different conditions. ReHo has already been used extensively to describe abnormal connectivity patterns in patients with neurological (Cao *et al.*, 2006; Wu *et al.*, 2009) and psychiatric disease (Liu *et al.*, 2006), as well as normal ageing subjects (Richiardi *et al.*, 2011).

To our knowledge, no rs-fMRI study has been conducted on sleep apnea patients, so our study could contribute to the neuropathophysiological characterization of sleep apnea impact on brain spontaneous functional organization. Specifically, we wanted to investigate: (1) if there are changes in fMRI functional connectivity in OSA patients; (2) if these changes could resample volumetric or metabolic findings that have been published recently; and (3) if individual local connectivity values (ReHo) in specific regions could correlate with pathology severity indexes. To ensure a better overview of possible differences between patients and healthy controls we also performed multivariate pattern analysis (MVPA) using ReHo values, thereby attempting to overcome all the limitations related to massive univariate statistical analysis of magnetic resonance imaging (MRI)–fMRI data.

METHODS

Participants

Thirty-eight participants were studied: 19 never-treated OSA patients, 16 men and three women and 19 age- and education-matched healthy controls (Table 1). All participants were right-handed, drug-naive monolingual native Italian speakers. Participants had no evidence of neurological and psychiatric disorders, or hypertension, diabetes, obesity and other sleep disorders. Inclusion criteria for OSA patients were: (1) diagnosis of OSA with an apnea–hypopnea index (AHI) >30; and (2) age between 30 and 55 years.

Healthy controls had an AHI <5, normal neurological physical examination, regular sleep–wake pattern, absence of sleep disorders (restless legs syndrome and periodic limb movements, insomnia or excessive day sleepiness, parasomnias) investigated by a sleep interview performed by a sleep medicine specialist and through a sleep diary/questionnaire. Participants were excluded if they demonstrated: (1) symptoms of cognitive deterioration (as indicated by a score at Mini-Mental State Examination below 24); or (2) brain structural abnormalities, as shown by evaluation of MR images by an experienced neuroradiologist. All participants, including healthy controls, reported regular sleep–wake schedules based on daily sleep diaries with an average total sleep time (TST) of 7.1 ± 1.2 h in the week prior to the study. All participants provided written informed consent to the experimental procedure, which was approved previously by the local ethics committee. Patients and control subjects were submitted to full nocturnal polysomnography (PSG), MRI–fMRI), sleepiness and mood evaluation.

Table 1 Demographic and clinical characteristic of study participants; P-value refers to two-tailed independent Student's t-test; means ± standard deviation are reported

Characteristic	Patients (n = 19)	Controls (n = 19)	P-value
Age (years)	43.2 ± 8	41 ± 6	0.78
Gender	16 M; 3 F	14 M; 5 F	–
Education (years)	12.3 ± 3	13.3 ± 2	0.53
Body mass index (BMI)	30.3 ± 2	25.7 ± 3	0.14
Epworth sleepiness scale	14.4 ± 3	4.8 ± 3	0.01
Beck depression inventory	6 ± 2	5 ± 2	0.34
Pathology length (years)	6.5 ± 3	–	–
Apnea–hypopnea index (AHI)	36.3 ± 13	–	–
Oxygen desaturation index (ODI)	34.5 ± 13	–	–
Oxygen saturation (min)	76.2 ± 9	–	–
Desaturation time (<90%)	11.3 ± 6	–	–
Apnea duration (mean)	27.5 ± 7	–	–
Hypopnea duration (mean)	31.8 ± 9	–	–
Apnea duration (max)	87.2 ± 37	–	–
Hypopnea duration (max)	103.1 ± 34	–	–
OSA severity (L=light; M=medium; S=severe)	1 L; 2 M; 16 S	–	–

F, female; M, male; OSA, obstructive sleep apnea.

PSG acquisition and data analysis

The week before sleep studies/PSG began, subjects were asked to complete a sleep diary (and not to drink alcohol or caffeinated beverages on the day before). OSA patients and controls underwent PSG/Holter the night before functional scanning, using a Sonnoscreen plus (16 channels) (Somnomedics, Bellusco, MI, Italy) or a Somnologica system (Embla). Overnight polysomnography was performed using a 4-channel electroencephalogram (EEG; C3/A2, C4/A1, O1/A2, O2/A1), 4-channel electro-oculogram (EOG), electromyogram (EMG; submental, intercostal and anterior tibialis muscles) and an electrocardiogram with surface electrodes. A thermistor (for monitoring nasal airflow), a nasal air pressure monitor, an oximeter (for measuring oxygen saturation), piezoelectric bands (for determining thoracic and abdominal wall motion) and a body position sensor were also attached to the patients.

Subjects were recorded on videotape using an infrared video camera and were observed continuously by a polysomnography technician. Subjects went to bed at 23:00 hours and were awakened at 07:00 hours. Sleep architecture was scored in 30-s epochs, and sleep staging was interpreted according to the criteria of the American Academy of Sleep Medicine. AHI was defined as the number of apnea and hypopnea events per hour of sleep. An obstructive apnea was defined as a $\geq$ 90% drop of respiratory amplitude lasting at least 10 s, associated with continued or increased inspiratory effort. A hypopnoea was defined as a 30% drop of respiratory amplitude lasting $\geq$ 10 s, associated with repeated respiratory effort and (arousals or) oxygen saturation drops of $\geq$ 4%. Oxygen desaturation index (ODI) was defined as the number of desaturation events per hour of sleep. A desaturation was defined as $\geq$ 4% drop of oxygen saturation and a minimum interval of

3 s. The time of oxygen saturation (SpO2) below 90% during total sleep, the lowest nocturnal oxygen saturation (SpO2) value and the mean of the lowest peaks of SpO2 were also recorded.

Assessment of excessive daytime sleepiness (EDS)

The Epworth Sleepiness Scale (ESS) was used to assess subjective sleepiness. Objective sleepiness was evaluated by multiple sleep latency test (MSLT). In brief, this consists of a series of five 20-min naps at 2-h intervals in the morning and afternoon. Patients are asked to try to sleep in a dark room with an EEG, EOG and EMG montage. The mean of the individual latencies to sleep onset from lights off was calculated in five nap trials.

Neuroradiological acquisition

All patients underwent an extensive neuroradiological examination performed using a 1.5 Tesla Philips Intera Scanner (Philips Medical Systems, Best, the Netherlands). For study purposes, the following sequences were taken into account: T1-weighted fast field echo (FFE) 1-mm-thick axial images of the entire brain (TE = 4.6 ms, TR = 30.00 ms, flip angle = 30.00, FOV = 250 mm, matrix 256 × 256, slice number = 150), fMRI BOLD sequence acquired during the rest condition (TR/TE 2500 40 ms^{-1}, 200 scans, 23 interleaved slices, 1-mm gap). Patients were asked to keep their eyes open and not to focus their thoughts on any particular topic. Only subjects with a negative response to lesion detection on T1–T2-weighted images were entered into the statistical analysis, while also considering the prevalence of silent cerebrovascular lesions reported in patients with moderate–severe OSA (Nishibayashi *et al.*, 2008).

fMRI data preprocessing and statistical analysis

Functional image preprocessing and statistical analyses were carried out using SPM8 software (Statistical Parametric Mapping; http://www.fil.ion.ucl.ac.uk/spm/), REST and the DARTEL toolbox for SPM, MATLAB version 7.5 (MathWorks, Natick, MA, USA). The first five volumes of functional images were discarded to allow for steady-state magnetization. Briefly, images were slice-time corrected, realigned, resliced to correct for head motion, coregistered with the structural images. To ensure a clearer normalization process, we used the DARTEL toolbox to create customized templates and tissue priors for grey matter, white matter and cerebrospinal fluid (CSF) of all subjects' T1-weighted images, and consequently used these optimized templates to newly segment both patients' and controls' structural images. Images were spatially normalized to the MNI T1 template (ICBM 152, Montreal Neurological Institute standard T1-weighted template) and hidden Markov random field model was applied in order to remove isolated voxels. The customized prior images and T1-weighted template were smoothed using an 8-mm full width at half maximum isotropic Gaussian kernel (FWHM IGK). For multivariate analysis, performing normalization on the whole data set violates train/test separation, and classification results are likely to be slightly optimistic. However, because no aberrant brain morphology was observed in the group this effect is likely to be minimal, because no single brain on its own will have a disproportionate effect on the group template. All functional volumes were band pass-filtered at 0.01 Hz <f <0.08 Hz to reduce low-frequency drift and physiological high-frequency respiratory and cardiac noise (Biswal *et al.*, 2010).

ReHo calculation

ReHo assumes that a given voxel time–course is temporally similar to that of its neighbours. The definition of each voxel's ReHo depends directly on the neighbours' cluster size, and is consequently an expression of local coherence at different spatial scales. Here we used Kendall's coefficient of concordance (KCC) to measure ReHo of each voxel in the brain by applying a cluster size of 26 voxels. Then, we obtained KCC map for each participant and proceeded to test for differences between OSA and control subjects. The KCC was calculated according to the following formula (Zang *et al.*, 2004):

$$W = \frac{\sum (R^i)^2 - n(\bar{R})^2}{1/12 K^2 (n^3 - n)},$$

where W is the KCC among given voxels, ranging from 0 to 1, Ri is the rank sum of the ith time-point; R = [(n + 1)K]/2 is the mean of the Ri, K is the number of time–series within a measured cluster (n = 27; one given voxel plus the others inside the cluster) and n is the number of ranks (corresponding to time-points; 200–5 = 195 ranks after discarding the first five volumes). Individual ReHo maps were generated by calculating the KCC value for every voxel throughout the whole brain. For standardization purposes, each individual ReHo map was divided by that subject's global mean brain KCC value, obtaining the mReHo maps used for statistical analysis. Then, to reduce noise and residual differences in gyral anatomy, the data were smoothed with a Gaussian filter of 6-mm FWHM (Zou *et al.*, 2009).

Univariate analysis

Regional homogeneity

First, in order to highlight the characteristic regional homogeneity spatial pattern of each participant group, a one-sided one-sample *t*-test ($P < 0.05$, false discovery rate correction [FDR]) was performed. ReHo maps in OSA and control groups were then compared on a voxelwise basis using a two-sample t-test and a customized explicit mask obtained from patients' and controls' unmodulated grey matter tissue maps. Results were displayed with an FDR-corrected threshold of $P < 0.05$, using a Monte Carlo simulation where the probability of false-positive detection takes into account both the individual voxel probability threshold and voxel cluster size (cluster connection radius 4 mm, individual voxel threshold probability 0.01, 1000 iterations, FWHM=6 mm, with mask). To exclude the effect of confounding covariate on ReHo values, age, gender, total brain volume and BMI were included as covariates in the analysis.

Polysomnographic and functional MRI data correlational analysis

To explore whether individual ReHo changes with OSA severity, an all-brain voxelwise correlation analysis of ReHo and AHI, TA<90, Sa02 min was performed in OSA patients. Moreover, sleepiness (ESS) was also included as an informative marker of sleep fragmentation. The results were corrected for multiple comparisons to a significance level of $P < 0.05$ by combining individual voxel *P*-value (<0.01) with cluster size (>41 voxels) through the Monte Carlo simulations described above.

Multivariate analysis

ReHo

The mean ReHo values were extracted from each anatomical regions of interest (ROI) of the *anatomical automatic labelling* (AAL) atlas (n = 90) and imported into 38 × 90 (subjects × vertexes) matrices. Through a multivariate pattern analysis classification process (leave-one-out cross-validation), several generative and discriminative algorithms were tested: naive Bayes (NB), logistic (LG), simple logistic (SLG), sequential minimal optimization (SMO), logistical model *tree (*LMT), functional tree (FT), J48, naive Bayes tree (NBT), simple cart (SC), random tree (RT) and random forest (RF)

with 301 trees. All these classifiers are implemented in Weka software (Hall *et al.*, 2009). For visualization purposes, the best-performing algorithms (correct classification percentage) were selected and a vector of the most discriminative features (brain regions) were calculated. Only features that overcame the 90 ° percentile were plotted on a three-dimensional glass brain in order to show brain areas that discriminate OSA patients more clearly from healthy controls in terms of local ReHo. However, the pattern is multivariate, and this graphic representation shows only the regions that carry most of the discriminative weight–that is, they are relatively more important to forming the decision boundary.

Results of univariate analysis

*Resting-state cerebral connectivity changes: regional homogeneity*

ReHo maps of both groups are shown in Fig. 1. Control subjects showed a default mode network alike regional homogeneity distribution. A near to absence reduction of the typical default mode network frontal component could be seen in the spontaneous synchronization map of OSA patients. Whole brain analysis indicated that OSA subjects displayed significantly decreased ReHo values in multiple areas (degree of freedom, Dof=37), including the bilateral parietal lobes (highest T values in right superior parietal lobule=−4.24) and precuneus, left inferior and middle frontal gyrus, left postcentral gyrus, right parahippocampal gyrus, left inferior and middle temporal gyrus, left fusiform gyrus, bilateral rectal gyrus and cerebellum (lobule VII Crus I, lobule I, lobule IV). Increased ReHo regions were situated bilaterally in the posterior part of the brain, namely in the right cingulated cortex (highest T values=4.62), right cuneus, right calcarine gyrus, bilateral lingual gyrus, left middle occipital gyrus, left middle and superior temporal gyrus and left globus pallidus. Detailed results are shown in Fig. 2 (*P* < 0.05, Monte Carlo correction) and Table 2.

Results of multivariate analysis

ReHo analysis detected a pattern of brain regions able to discriminate patients and healthy controls with a correct classification rate of 82.25% using a sequential minimal optimization function (confidence interval [CI]: 0.6748–0.91; accuracy=0.81; sensitivity=0.73; specificity=0.93; area under the curve [AUC] 0.96) and 77.5% using a naive Bayes classifier (CI: 0.63–0.87; accuracy=0.76; sensitivity=0.82; specificity=0.74; AUC 0.86) (Fig. 3). Specifically, the classifier weights were relatively higher in parietal gyri, indicating that these regions influence the decision to hyperplane more, relative to other regions with lower weights. In other words, a small change in the value of the signal in these regions will change the value of the decision function more than the same magnitude of change in the same number of voxels having a lower classifier weight, thus impacting the classification result more.

Correlations between clinical and functional data

The results of the correlation analysis between ReHo maps and clinical data are showed in Fig. 4 and Table 3. We found a global trend of negative correlations between pathology severity and local connectivity in right hemisphere posterior brain regions, especially the mesial part of occipital and parietal lobes. Moreover, the increase of oxygen saturation (SpO2) time below 90% during total sleep time also corresponds to a decrease of regional homogeneity in the right middle frontal gyrus. It should be noted that, in contrast to other PSG AHI and T<90 °, a higher minimum saturation value (Sa02 min) corresponds to a worse condition, so its correlation with posterior regions appears reversed, i.e. positive. A consequent increase of local coherence to pathology worsening has been found mainly in the left hemisphere regions, such as inferior and middle temporal lobe, fusiform gyrus, rolandic operculum, gyrus rectus, orbital and parahippocampal gyri. Finally, sleepiness values (ESS) seem to correlate negatively with spontaneous local
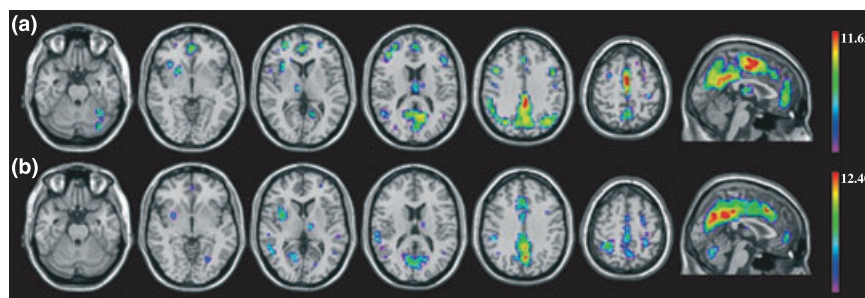
Figure 1. Intrinsic brain local coherence profiles. The figure shows regional homogeneity mapping across healthy controls (a) and obstructive sleep apnea (OSA) patients (b) (one-sample *t* test; *P* < 0.001, false discovery rate correction). Significant regional homogeneity (ReHo) clusters observed in both groups include default mode network (DMN) areas, such as precuneus and posterior cingulate cortex. OSA patients did not show DMN bilateral parietal and frontal (mainly middle prefrontal cortex) nodes. Radiological convention.
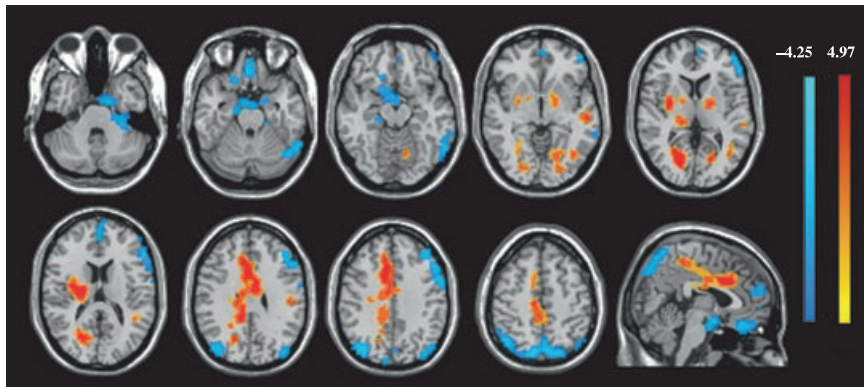
Figure 2. Regional homogeneity (ReHo) comparison results. The figure represents differences in regional homogeneity values between obstructive sleep apnea (OSA) patients and healthy controls ($P < 0.05$, false discovery rate correction). T-score bars on the right indicate increased and decreased (hot and cold colour-coded) regional homogeneity, respectively, in OSA patients. Radiological convention.

coherence of bilateral inferior temporal regions and rectus gyri, with an increase in the left rolandic, supramarginal, precentral and postcentral gyri.

DISCUSSION

In the present study we originally compared resting-state fMRI data from a group of patients suffering from OSA with an age–and gender-matched control group. We performed both univariate and multivariate analyses using a voxel-based local coherence index (RoHo) (Zang *et al.*, 2004), aimed at describing locally circumscribed alterations in spontaneous brain functioning. We found a significant pattern of cortical and subcortical abnormal local connectivity in OSA patients that suggests an overall rearrangement of right hemisphere connectivity, with a major affect on somatosensory and motor regions, and a bilateral increase of spontaneous local coherence into thalamic nuclei. Both results suggest how long-term exposure to sleep apnea syndrome could induce significant changes in brain spontaneous functioning, especially in those regions involved in the arousal system and motor/sensorial aspects of the respiratory tract.

Local coherence changes in the right hemisphere

First, our findings seem to support a more pronounced pattern of decreased connectivity in the right hemisphere, evidence that confirms previous results from functional studies using PET as well as *in-vivo* anatomical studies highlighting a major affliction of the right hemisphere using both VBM (Yaouhi *et al.*, 2009) and surface-based techniques (Torelli *et al.*, 2011). Conversely, we did not find a decrease of local connectivity restricted to the frontal lobe, as in the PET study by (Antczak *et al.*, 2007), but also in posterior brain regions such as parietal and superior occipital lobes. These results reflect evidence of an EEG slowing in the occipital and parietal areas documented in OSA patients, characterized by an increase in theta and delta power

compared to controls (Morisson *et al.*, 1998; Xiromeritis *et al.*, 2011). Moreover, a fronto-parietal activity reduction compared to controls has been also found in an fMRI study involving attention tasks (Ayalon *et al.*, 2009), and reduced perfusion of the left parietal region has been also found in a single photon emission computed tomography (SPECT) study (Ficker *et al.*, 1997). Hemispheric differences in spontaneous BOLD fluctuations could also be linked to the diurnal impact of nocturnal "EEG arousal" (EEGA), a transient electrical phenomenon detectable through EEG and EMG recordings, that does not generally result in natural awakening but contributes hugely to sleep fragmentation (Swarnkar *et al.*, 2006). A study by (Swarnkar *et al.*, 2007) suggested how, during EEGA, there is an interhemispheric asynchrony, with a spectral correlation coefficient reduction between the two hemispheres during the non-rapid eye movement (NREM) stage and its total disappearance during the REM sleep stage. The persistence of this condition for years, combined with the pathological severity of our patients, could be a possible explanation of this interhemispheric functional connectivity inequality during wakefulness.

Somatosensory and motor regions increased coherence

Our results also suggest a pattern of increased intrinsic connectivity in bilateral pre-central and postcentral gyri. This altered pattern of brain activity in motor and somatosensory cortices could be linked to an increased mechanical effort that may occur during pathological arousal in sleep, with an immediate restoration of breathing muscle tone to waking levels. Moreover, functional MRI in humans has revealed a significant activation increase in the posterior parietal cortex during transition from unconscious to conscious breathing (Smejkal *et al.*, 1999). OSA microarousal represents repetitive and incomplete nocturnal transition from sleep to wakefulness, so persistence through time could have induced this stable local coherence rearrangement in the parietal cortex.

Table 2 Regional homogeneity (ReHo) group comparison results, showing clusters of decreased and increased regional homogeneity value in sleep apnea patients compared to controls. Voxels count, MNI coordinates and peak T-values are reported for the most represented region of each cluster, with other regions included in the cluster listed sequentially. Results refer to t-statistics obtained using Monte Carlo simulation multiple comparisons correction at P < 0.05

Location	Voxel	Decreased ReHo in OSA patients Peak t-value MNI coordinates			Peak t-value (Dof=37)
		x	y	z	
Right superior parietal lobule	820	9	−81	51	−4.24
Right precuneus					
Right inferior parietal lobule					
Right middle occipital gyrus					
Left superior parietal lobule					
Left precuneus					
Left middle occipital gyrus					
Right inferior frontal gyrus (P. triangularis)	360	−48	48	6	−3.87
right inferior frontal gyrus (P. opercularis)					
Right middle frontal gyrus					
Right postcentral gyrus					
Right pre-central gyrus					
Right parahippocampal gyrus	359	6	−3	−21	−4.25
Left fusiform gyrus					
Right inferior frontal gyrus (P. orbitalis)					
Right olfactory cortex					
Left amygdala					
Right inferior temporal gyrus	134	−57	−54	−21	−3.83
Right cerebellum					
Right middle temporal gyrus					
Right inferior occipital gyrus					
Left cerebellum	79	−30	−33	−39	−3.66
Right rectal gyrus	78	3	33	−21	−3.8
Left rectal gyrus					
Left superior medial gyrus	72	0	54	21	−3.59
Increased ReHo in OSA patients					
Right middle cingulate cortex	1275	9	−15	42	4.62
Right posterior cingulate cortex					
Left anterior cingulate cortex					
Left thalamus	410	15	−15	6	4.38
Right thalamus	398	−12	−18	9	4.19
Right calcarine gyrus	368	21	−72	6	4.07
Right cuneus					
Right lingual gyrus					
Left lingual gyrus	115	−21	−66	3	3.99
Left middle occipital gyrus	69	−39	−69	0	3.95
Left superior temporal gyrus					
Left globus pallidus	68	−15	−3	3	3.53
Left middle temporal gyrus	46	−54	−24	−3	3.53
Left rolandic operculum	41	−48	−12	24	3.56
Left postcentral gyrus					

MNI, Montreal Neurological Institute; OSA, obstructive sleep apnea.

Frontal lobe findings

Frontal lobe regional homogeneity alterations substantially reflect neuropsychological findings concerning worsening of sustained attention and cognitive flexibility performance in OSA patients. It is possible that the hypoxias and hyper-capnias caused by apneic episodes result in local disruption in the regulation of sleep in frontal lobes, as already documented in animal studies (Piantadosi *et al.*, 1997), or that repetitive cortical arousal could induce a frontal

hyperperfusion, as documented in a SPECT study (Ficker *et al.*, 1997).

Thalamic coherence increase at rest

Our most intriguing result refers to the increased regional homogeneity of bilateral thalamic nuclei. Until now only a few studies have reported alteration in these deep brain structures (Joo *et al.*, 2010; Yaouhi *et al.*, 2009), even though a thalamus role in sleep-related neurological disorder
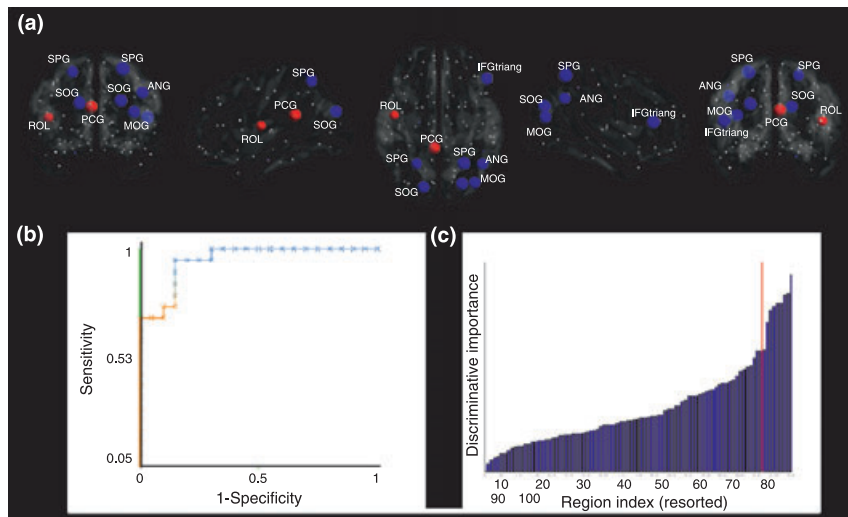
Figure 3. Results of functional multivariate analysis. Panel (a) represents the relatively more discriminative brain areas (>90th percentile) between obstructive sleep apnea (OSA) patients and controls in terms of regional homogeneity. Blue and red spheres, respectively, represent areas with diminished and augmented regional homogeneity in OSA patients with respect to controls. This graphic representation shows only the regions that carry most of the discriminative weight–that is, those that are relatively more important to forming the decision boundary. (b,c) Receiving operator curve (ROC) results for OSA classification through regional homogeneity (ReHo) values, and distribution with 90th percentile cut-off (red line). ANG: angular gyrus; IFGtriang: inferior frontal gyrus triangular part; MOG: middle occipital gyrus; PCG: posterior cingulate gyrus; ROL: rolandic operculum; SOG: superior occipital gyrus; SPG: superior parietal gyrus.
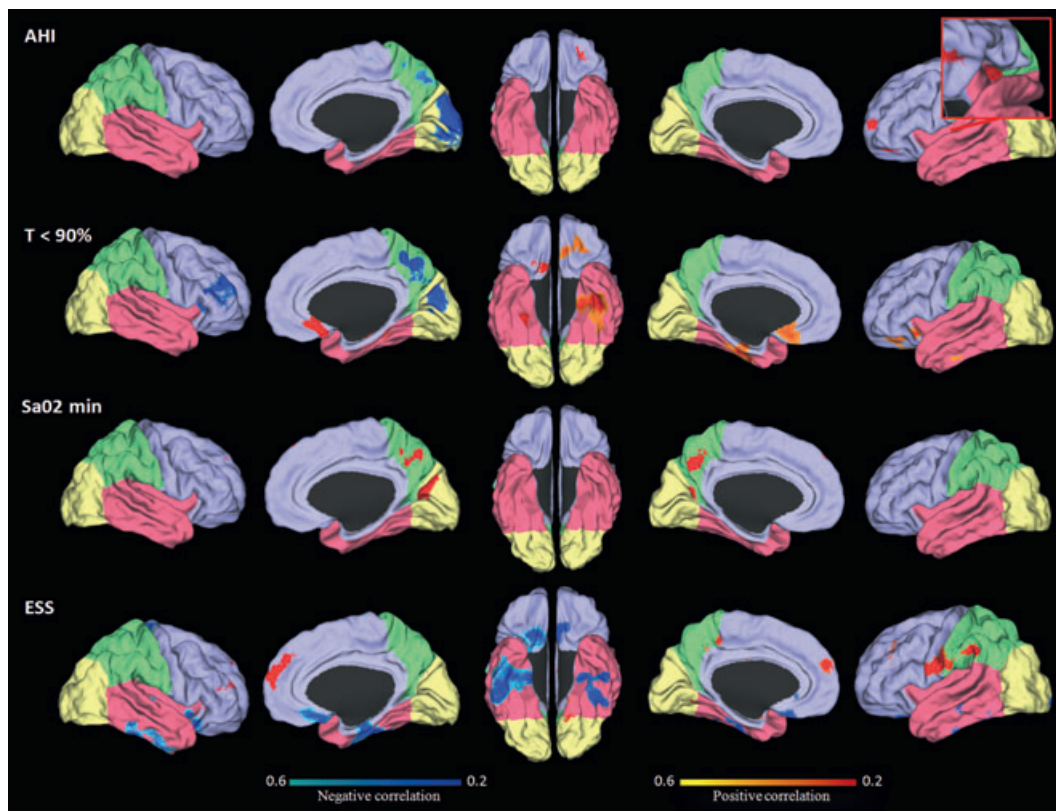
Figure 4. Results of polysomnographic (PSG)–regional homogeneity (ReHo) correlational analysis. Red and blue clusters represent positive and negative correlation (Pearson's correlation coefficient, $P < 0.05$, Monte Carlo correction) between regional homogeneity values and clinical indexes in obstructive sleep apnea (OSA) patients (AHI: apnea–hypopnea index; Sa02 min: lowest nocturnal oxygen saturation [SpO2] value; T<90 °: time of oxygen saturation [SpO2] below 90% during total sleep time; ESS: Epworth Sleepiness Scale). Radiological convention.

Table 3 Correlations between polysomnographic (PSG) data and regional homogeneity values in obstructive sleep apnea (OSA) patients, showing clusters of significant correlation between PSG data and whole brain regional homogeneity values; results refer to Pearson's r-statistics obtained using Monte Carlo simulation multiple comparisons correction at P < 0.05

Correlation clusters location	Voxels	MNI coordinates			Peak r-value (n = 38)
		x	y	z	
AHI-positive correlations	42				
Left rolandic operculum		−42	−22	23	0.65
AHI-negative correlations					
Right cuneus	66	3	−103	26	−0.56
Right superior occipital gyrus		12	−106	23	−0.53
T<90% positive correlations	357				
Left parahippocampal gyrus		−30	−16	−25	0.64
Left middle temporal gyrus		−51	−25	−7	0.62
Left fusiform gyrus		−39	−13	−31	0.61
Left inferior temporal gyrus		−45	−25	−19	0.54
Right rectus gyrus		3	33	−21	0.5
T<90% negative correlations	48				
Right middle frontal gyrus		30	41	29	−0.65
Right precuneus		3	−67	56	−0.62
Right superior occipital gyrus		15	−85	32	−0.61
Right cuneus		9	−88	29	−0.54
Sa02min positive correlations	143				
Right precuneus		3	−61	47	0.65
Left precuneus		−9	−58	65	0.64
Right cuneus		−12	−76	41	0.62
Right calcarine gyrus		6	−76	26	0.6
Right lingual gyrus		18	−67	5	0.58
Left calcarine gyrus		−24	−73	14	0.54
ESS-positive correlations	263				
Left postcentral gyrus		−30	−40	59	0.62
Left precuneus		−15	−58	50	0.62
Left precentral gyrus		−27	−28	62	0.61
Left rolandic operculum		−63	5	14	0.6
Left supramarginal gyrus		−63	−40	44	0.59
Left middle temporal gyrus		−42	−61	17	0.55
ESS-negative correlations	890				
Right parahippocampal gyrus		15	2	−19	−0.63
Right insula lobe		39	11	−4	−0.61
Right paracentral lobule		9	−34	80	−0.61
Right hippocampus		24	−16	−16	−0.6
Left inferior temporal gyrus		−51	−55	−19	−0.57
Left middle temporal gyrus		−63	−25	−4	−0.54
Left fusiform gyrus		−45	−49	−19	−0.51

AHI, apnea–hypopnea index; ESS, Epworth Sleepiness Scale; MNI, Montreal Neurological Institute.

neurophysiology seems extremely plausible for several reasons, particularly for sleep apnea. Considering the fundamental role of the thalamus into the arousal mechanism and sleep–wake transition process (Jones, 2003), an alteration of its spontaneous diurnal behaviour could represent the effect of an aberrant overstimulation during the night, while choke sensation and increased breathing effort components of apneic episodes induce brief and partial cortical arousal, i.e. microarousal. These incomplete electrical cortical reactivations, repeated several times during the night and probably experienced through years, could also have generated an aberrant thalamic hyperactivation during the rest condition.

Pathology severity link with brain spontaneous functioning

The correlation between clinical scores and ReHo values highlights the usefulness of this functional connectivity measure in detecting the pathological impact on the brain, clearly supporting the different hemispheric illness response. An increase in sleep apnea severity, represented by PSG indexes such as AHI and oxygen saturation time below 90% during the night, seems to correspond to a reduction in local synchronization of right parietal, occipital and frontal lobes in sleep apnea patients. At the same time, contralateral balancing seems to appear, with an opposite

trend of increased local coherence in left temporal and frontal lobes.

Sleepiness seems to be anticorrelated with bilateral brain regions deputed to memory, such as hippocampus and parahippocampal, fusiform and temporal gyri, a finding that sustains the reduction of memory performance already stressed in several studies concerning OSA (Bruin and Bagnato, 2010; Canessa *et al.*, 2011).

OSA multivariate profile

Multivariate analysis has demonstrated its undeniable usefulness by uncovering a widespread pattern of alterations in functional imaging data, confirming the right-lateralized decreased of local coherence and an increase in the left pre-central gyrus. Even in the atlas-based version adopted here, this approach could be expanded to the multivariate classification of OSA patients through different MRI data information, aiming at the identification of most informative biomarkers for sleep apnea between volumetric (grey matter volume, thickness or concentration), structural (fractional anisotrophy, mean diffusivity) and functional (ReHo, functional connectivity, network properties) indexes.

CONCLUSIONS

Our study confirms previous EEG and task-fMRI-based knowledge of the impact of the sleep apnea condition on the brain, suggesting that a global rearrangement is even possible during diurnal resting-state brain functioning. Different hemispheric roles into sleep processes and a possible thalamus key role in OSA neurophysiopathology are intriguing issues that future work should attempt to clarify.

Future directions

In order to evaluate fronto-parietal dysfunction and sleepiness impact on brain activity, a data-driven approach should be applied in the OSA rs-fMRI data set, trying to correlate activity within the attentional network (AN) and the interplay between the AN and default mode network (DMN).

ACKNOWLEDGEMENTS

DISCLOSURE STATEMENT

All authors report no conflicts of interest.

REFERENCES

Algin, O., Gokalp, G., Ocakoglu, G., Ursavas, A., Taskapilioglu, O. and Hakyemez, B. Neurochemical–structural changes evaluation of brain in patients with obstructive sleep apnea syndrome. *Eur. J. Radiol.*, 2012, 81: 491–495.

Antczak, J., Popp, R., Hajak, G., Zulley, J., Marienhagen, J. and Geisler, P. Positron emission tomography findings in obstructive sleep apnea patients with residual sleepiness treated with continuous positive airway pressure. *J. Physiol. Pharmacol.*, 2007, 58 (Suppl. 5): 25–35.

Ayalon, L., Ancoli-Israel, S., Klemfuss, Z., Shalauta, M.D. and Drummond, S.P. Increased brain activation during verbal learning in obstructive sleep apnea. *Neuroimage*, 2006, 31: 1817–1825.

Ayalon, L., Ancoli-Israel, S., Aka, A.A., McKenna, B.S. and Drummond, S.P. Relationship between obstructive sleep apnea severity and brain activation during a sustained attention task. *Sleep*, 2009, 32: 373–381.

Biswal, B.B., Mennes, M., Zuo, X.N. *et al.* Toward discovery science of human brain function. *Proc. Natl Acad. Sci. USA*, 2010, 107: 4734–4739.

Bruin, P.F. and Bagnato, M.C. Cognitive impairment in obstructive sleep apnea syndrome. *J. Bras. Pneumol.*, 2010, 36(Suppl. 2): 32–37.

Bulcun, E., Ekici, A. and Ekici, M. Quality of life and metabolic disorders in patients with obstructive sleep apnea. *Clin. Invest. Med.*, 2012, 35: E105.

Canessa, N., Castronovo, V., Cappa, S.F. *et al.* Obstructive sleep apnea: brain structural changes and neurocognitive function before and after treatment. *Am. J. Respir. Crit. Care Med.*, 2011, 183: 1419–1426.

Cao, Q., Zang, Y., Sun, L. *et al.* Abnormal neural activity in children with attention deficit hyperactivity disorder: a resting-state functional magnetic resonance imaging study. *NeuroReport*, 2006, 17: 1033–1036.

Drummond, S.P., Brown, G.G., Gillin, J.C., Stricker, J.L., Wong, E.C. and Buxton, R.B. Altered brain response to verbal learning following sleep deprivation. *Nature*, 2000, 403: 655–657.

Ficker, J.H., Feistel, H., Moller, C. *et al.* Changes in regional CNS perfusion in obstructive sleep apnea syndrome: initial SPECT studies with injected nocturnal 99mTc-HMPAO. *Pneumologie*, 1997, 51: 926–930.

Gama, R.L., Távora, D.G., Bomfim, R.C. *et al.* Sleep disturbances and brain MRI morphometry in Parkinson's disease, multiple system atrophy and progressive supranuclear palsy: a comparative study. *Parkinsonism Relat Disord*, 2010, 16: 275–275.

Hall, M., Frank, E., Holmes, G., Pfahringer, B., Reutemann, P. and H. Witten, I.H. The WEKA data mining software: an update. *SIGKDD Explorations*, 2009, 11: 10–18.

Horner, R.L. Pathophysiology of obstructive sleep apnea. *J. Cardiopulm. Rehabil. Prev.*, 2008, 28: 289–298.

Jones, B.E. Arousal systems. *Front. Biosci.*, 2003, 8: s438–s451.

Joo, E.Y., Tae, W.S., Lee, M.J. *et al.* Reduced brain gray matter concentration in patients with obstructive sleep apnea syndrome. *Sleep*, 2010, 33: 235–241.

Liu, H., Liu, Z., Liang, M. *et al.* Decreased regional homogeneity in schizophrenia: a resting state functional magnetic resonance imaging study. *NeuroReport*, 2006, 17: 19–22.

Macey, P.M., Kumar, R., Woo, M.A., Valladares, E.M., Yan-Go, F.L. and Harper, R.M. Brain structural changes in obstructive sleep apnea. *Sleep*, 2008, 31: 967–977.

Morisson, F., Lavigne, G., Petit, D., Nielsen, T., Malo, J. and Montplaisir, J. Spectral analysis of wakefulness and REM sleep EEG in patients with sleep apnoea syndrome. *Eur. Respir. J.*, 1998, 11: 1135–1140.

Nishibayashi, M., Miyamoto, M., Miyamoto, T., Suzuki, K. and Hirata, K. Correlation between severity of obstructive sleep apnea and prevalence of silent cerebrovascular lesions. *J. Clin. Sleep Med.*, 2008, 4: 242–247.

Piantadosi, C.A., Zhang, J., Levin, E.D., Folz, R.J. and Schmechel, D.E. Apoptosis and delayed neuronal damage after carbon monoxide poisoning in the rat. *Exp. Neurol.*, 1997, 147: 103–114.

Richiardi, J., Eryilmaz, H., Schwartz, S., Vuilleumier, P. and Van, D.V. Decoding brain states from fMRI connectivity graphs. *Neuroimage*, 2011, 56: 616–626.

Smejkal, V., Druga, R. and Tintera, J. Control of breathing and brain activation in human subjects seen by functional magnetic resonance imaging. *Physiol. Res.*, 1999, 48: 21–25.

Swarnkar, V., Abeyratne, U.R. and Karunajeewa, A.S. Left-right information flow in the brain during EEG arousals. *Conf. Proc. IEEE Eng Med. Biol. Soc.*, 2006, 1: 6133–6136.

Swarnkar, V., Abeyratne, U.R. and Hukins, C. Inter-hemispheric asynchrony of the brain during events of apnoea and EEG arousals. *Physiol. Meas.*, 2007, 28: 869–880.

Torelli, F., Moscufo, N., Garreffa, G. *et al.* Cognitive profile and brain morphological changes in obstructive sleep apnea. *Neuroimage*, 2011, 54: 787–793.

Wu, T., Long, X., Zang, Y. *et al.* Regional homogeneity changes in patients with Parkinson's disease. *Hum. Brain Mapp.*, 2009, 30: 1502–1510.

Xiromeritis, A.G., Hatziefthimiou, A.A., Hadjigeorgiou, G.M., Gourgoulianis, K.I., Anagnostopoulou, D.N. and Angelopoulos, N.V. Quantitative spectral analysis of vigilance EEG in patients with obstructive sleep apnoea syndrome: EEG mapping in OSAS patients. *Sleep Breath.*, 2011, 15: 121–128.

Yaouhi, K., Bertran, F., Clochon, P. *et al.* A combined neuropsychological and brain imaging study of obstructive sleep apnea. *J. Sleep Res.*, 2009, 18: 36–48.

Zang, Y., Jiang, T., Lu, Y., He, Y. and Tian, L. Regional homogeneity approach to fMRI data analysis. *Neuroimage*, 2004, 22: 394–400.

Zimmerman, M.E. and Aloia, M.S. A review of neuroimaging in obstructive sleep apnea. *J. Clin. Sleep Med.*, 2006, 2: 461–471.

Zou, Q., Wu, C.W., Stein, E.A., Zang, Y. and Yang, Y. Static and dynamic characteristics of cerebral blood flow during the resting state. *Neuroimage*, 2009, 48: 515–524.